Published in final edited form as:
J Muscle Res Cell Motil. 2011 March ; 31(0): 323–336. doi:10.1007/s10974-011-9238-9.

Biomechanics of the sarcolemma and costameres in single skeletal muscle fibers from normal and dystrophin-null mice

K. P. García-Pelagio,
Departamento de Bioquímica, Facultad de Medicina, Universidad Nacional Autónoma de México, Mexico, DF 04510, Mexico

R. J. Bloch,
Department of Physiology, University of Maryland, School of Medicine, 655 West Baltimore St., Baltimore, MD 21201, USA

A. Ortega, and
Departamento de Bioquímica, Facultad de Medicina, Universidad Nacional Autónoma de México, Mexico, DF 04510, Mexico

H. González-Serratos
Department of Physiology, University of Maryland, School of Medicine, 655 West Baltimore St., Baltimore, MD 21201, USA. Departamento de Fisiología, Facultad de Medicina, Universidad Nacional Autónoma de México, Mexico, DF 04510, Mexico

H. González-Serratos: hgonzale@umaryland.edu

Abstract

We studied the biomechanical properties of the sarcolemma and its links through costameres to the contractile apparatus in single mammalian myofibers of *Extensor digitorum longus* muscles isolated from wild (WT) and dystrophin-null (mdx) mice. Suction pressures (P) applied through a pipette to the sarcolemma generated a bleb, the height of which increased with increasing P. Larger increases in P broke the connections between the sarcolemma and myofibrils and eventually caused the sarcolemma to burst. We used the values of P at which these changes occurred to estimate the tensions and stiffness of the system and its individual elements. Tensions of the whole system and the sarcolemma, as well as the maximal tension sustained by the costameres, were all significantly lower (1.8–3.3 fold) in muscles of mdx mice compared to WT. Values of P at which separation and bursting occurred, as well as the stiffness of the whole system and of the isolated sarcolemma, were ~2-fold lower in mdx than in WT. Our results indicate that the absence of dystrophin reduces muscle stiffness, increases sarcolemmal deformability, and compromises the mechanical stability of costameres and their connections to nearby myofibrils.

Keywords

Muscle mechanics; Costamere; mdx; Superficial tension; Dystrophic muscle; Muscular dystrophy

Introduction

Costameres are structures at the sarcolemma of striated muscle fibers that align circumferentially with the Z disks and the M bands of the nearest myofibrils. Costameres maintain and coordinate the organization of the sarcolemma with the underlying contractile apparatus, while ensuring that distortions in the sarcolemma during isotonic contractions, that lead to shortening below the equilibrium length, are small and periodic (Bloch et al. 2002; Bloch and Gonzalez-Serratos 2003; Anastasi et al. 2008). They also organize membrane domains at the sarcolemma that are enriched in proteins, signaling molecules, ion channels and pumps, that are essential for proper physiological function of striated muscles (Brenman et al. 1995; Williams and Bloch 1999a; Oak et al. 2003; Ervasti 2003). They constitute an essential structure in the pathway for lateral force transmission from myofibrils through the sarcolemma to the extracellular matrix, and ultimately to the tendons (Bloch and Gonzalez-Serratos 2003). Defects in proteins at costameres can compromise muscle force production during contraction either directly, by reducing the efficiency of lateral force transmission, or indirectly, by increasing the chances that the sarcolemma will be weakened and damaged, resulting in degeneration or death of the myofiber (Reed and Bloch 2005; Blaauw et al. 2008). Many muscular dystrophies, associated with a profound weakness and fragility of myofibers (Barton 2006), have been linked to alterations in costameric proteins such as dystrophin (Hoffman et al. 1987; Williams and Bloch 1999b; Rybakova et al. 2000; Ervasti 2007), sarcoglycans (Nigro et al. 1996; Williams and Bloch 1999a; Lapidos et al. 2004), and dystroglycans (Ozawa 1998; Campbell and Stull 2003; Ayalon et al. 2008).

Dystrophin is a 427 kDa cytoskeletal protein enriched at costameres that is thought to connect the cytoskeleton to integral proteins of the plasma membrane (Porter et al. 1992; Ervasti and Campbell 1991, 1993; Williams and Bloch 1999a; Rybakova et al. 2000; Ursitti et al. 2004; Bhosle et al. 2006; Ervasti 2007; Stone et al. 2007), and through the membrane, to the basal lamina (Ohlendieck et al. 1991; Dmytrenko et al. 1993; Winder 1997; Campbell and Stull 2003; Beedle et al. 2007). Dystrophin and the proteins with which it associates at the plasma membrane, termed the dystrophin–glycoprotein complex, have been linked to different forms of muscular dystrophy. In particular, Duchenne and Becker muscular dystrophies are caused by mutations in the gene that encodes dystrophin, leading to its absence (Duchenne) or presence at the sarcolemma in reduced amounts or with impaired activity (Becker). Despite extensive study, the function of dystrophin and its biomechanical role at the sarcolemma, as well as how defects in the protein lead to muscular dystrophy, are still poorly understood (Nowak and Davies 2004; Claffin and Brooks 2008). Studies of the dystrophin-null mouse (*mdx*) model have shown that skeletal myofibers have disorganized costameres, which resemble those seen in biopsies of human muscular dystrophies (Porter et al. 1992; Ehmer et al. 1997; Minetti et al. 1998; Williams and Bloch 1999a; Reed and Bloch 2005). The location and structure of dystrophin suggest that it may play a role in the stability, stiffness and organization of the sarcolemma. Consistent with this, dystrophin mechanically reinforces the sarcolemma, protecting it from the membrane stresses developed during muscle contraction (Zubrzycka-Gaarn et al. 1988; Petrof et al. 1993; Blaauw et al. 2010).) Furthermore, some authors (Zubrzycka-Gaarn et al. 1988; Rybakova et al. 2000; Hutter et al. 1991) have shown that dystrophin is tightly attached to the

sarcolemma and that it remains attached to the sarcolemma when the latter is separated from the myofibrils. The absence of dystrophin in myotubes prepared from the *mdx* mouse has also been linked to a substantial reduction in cell stiffness (Pasternak et al. 1995).

Here we address the possibility that the absence of dystrophin results in a decrease in the transmission of passive force laterally, from the myofibrils to the sarcolemma, linked to changes in the properties of costameres. We use aspiration with a large bore micropipette to examine the biomechanical properties of the sarcolemma and costameres of wild type muscle fibers and *mdx*. This method has been used to measure the surface tension (Mitchison 1953), and the mechanical properties of cell membranes (Rand 1964; Evans and Yeung 1989; Hochmuth 2000; Zhang et al. 2007) including the sarcolemma of frog muscle fibers (Rapoport 1972). We examine the biomechanical properties of murine myofibers with the aim of determining the tension, stiffness and breaking point of the attachments between the sarcolemma and nearby myofibrils, which are likely to occur at costameres, and how these properties are affected by the absence of dystrophin. We report that the links between the contractile apparatus and costameres at the sarcolemma are stronger and stiffer in wild type than in *mdx* myofibers, and further, that the ability of the isolated sarcolemma to resist bursting is weakened in *mdx* mice. Preliminary accounts of these results have been published elsewhere (Garcia-Pelagio et al. 2006, 2008).

Materials and methods

Animals

WT mice (C57Bl/10ScSn, $n = 30$) and *mdx* (C57-Bl/10ScSn-DMD-*mdx*, $n = 18$) mice, from 7 to 11 weeks of age, were used. *WT* mice were purchased from The Jackson Laboratory (Bar Harbor, ME); *mdx* mice were raised in the Central Animal Facility of the University of Maryland, Baltimore. Before removal of muscles and dissection of myofibers, mice were euthanized by cervical dislocation without anesthesia. All experiments were in accordance with institutional guidelines for the care and welfare of laboratory animals.

Isolation of muscle fibers

Both EDL muscles were rapidly and carefully dissected under low magnification (×3), and placed in Kreb's solution, containing in mM: 135 NaCl, 5 KCl, 1 $MgCl_2$, 15 $NaHCO_3$, 11 glucose, 1 Na_2HPO_4 and 2.5 $CaCl_2$, equilibrated with 95% O_2 and 5% CO_2 to a pH of 7.0. Small bundles of approximately 100 fibers from the third toe muscle of the EDL muscle were isolated under a dissecting microscope. The bathing solution was replaced at least 3 times with Kreb's solution without Ca^{2+} and containing 15 mM EGTA. Bundles of fibers were transferred to relaxing solution, containing in mM: 185 $K(C_2H_5COO)$, 2.5 $Mg(CH_3COO)_2{\cdot}4H_2O$, 10 imidazole propionate, 2.5 Na_2ATP, 5 EGTA, pH 7.1. Single fibers were isolated from the bundles as previously described (Gonzalez-Serratos 1971). Dissecting in relaxing solution reduced the possibility of damaging myofibers. Similar preparations have been used to measure biomechanical properties in myofibers isolated from normal or mutant mice (Wieneke et al. 2000; Shah et al. 2004). The increase in myoplasmic Ca^{2+} concentration ($[Ca^{2+}]_i$) during exposure of myofibers to high K^+ concentrations, similar to the one we used here, is brief and transient, lasting only a few seconds, after

which $[Ca^{2+}]_i$ decreases to normal values (Caputo and Bolaños 1994), so prolonged increases in $[Ca^{2+}]_i$ do not occur. Low $[Ca^{2+}]_o$ has no deleterious effect on the biomechanical properties of isolated myofibers (Wieneke et al. 2000). We confirmed the latter by monitoring the health of the myofibers throughout our experiments, as described below.

General procedure

Isolated fibers were transferred to an experimental chamber containing relaxing solution, fixed to a stage of a compound Laborlux microscope (E. Leica Microsystems, Wetzlar, Germany). The optical part of the microscope was placed on an XY stage so that every part of the muscle cell could be visualized without disturbing the preparation or the subsequent placement of the glass micropipette. One tendon was clamped against a cover slip at the bottom of the chamber; the other tendon was fixed to a Narishige M-2 micromanipulator (Labtron Scientific Products, Farmingdale, NY), used to stretch the fiber. Photomicrographs were taken with a digital camera (Nikon D70, NY) through a ×10 eyepiece and ×40, N.A. 0.75 water immersion objective. The fiber was stretched to the desired average sarcomere length (SL), measured first by eye and then with Image J software (NIH, Bethesda, MD). The former measurements were made with a calibrated micrometer positioned inside a ×25 eyepiece. The diameter of the fiber was measured after SL was set. Experiments were done at 8°C, controlled by a GB32J36 thermistor (Fenwal Electronics, Framingham, MA), connected to a temperature controller (Yellow Springs Instrument Co., Inc, Ohio OH), which maintained the temperature through a two Peltier modulus (Midland Ross, Cambridge, MA). A micropipette (see below) was placed on the surface of the myofiber, and negative suction pressure (P) was applied.

Micropipettes

Micropipettes were made as described by Fonbrune (1949). Capillary tubes of 2 mm internal diameter were pulled to create a flat tip of internal opening of 0.50–0.66 times the diameter of the myofibers. In order to acquire precise measurements of the internal diameter of the micropipettes they were not fire polished because the curvature tip of these pipettes introduces microscopic distortions. The micropipettes do not damage the sarcolemma. The micropipette was connected to a set of manometers (see below) and was positioned on the surface of the myofiber with a micromanipulator (Leica Microsystems Inc., Bannockburn, IL).

Elastimetry

We modified the method of Rapoport (1972). Micropipettes were attached to 2 manometers, one filled with Hg and the other with perfluorinated polyether liquid (Miller-Stephenson, CT), with densities $\rho = 13.5$ and $\rho = 1.71$ g/cm^3, respectively (Fig. 1). The manometers were connected at one end to the micropipette and at the other to a syringe piston, and could be used independently. The manometers were first calibrated to zero suction pressure (P) by connecting the pipette to a 2 mm diameter capillary placed between the pipette and either one of the manometers. The capillary was filled with distilled water and graphite particles, and the tip of the micropipette was filled with bathing solution. The tips of the capillary

were placed at the level of the myofibers. Graphite particles in the capillary were observed with a compound microscope. Changes in the height of the manometers produced an inflow or outflow of the solution inside the capillary, resulting in the movement of graphite particles. When the graphite particles did not move, the applied pressure was zero. The existence of good seals (no leakage) between the micropipettes and the myofiber's sarcolemma was explored by applying suction pressure, P, which produced a bleb (Fig. 2). A constant value for P at a given manometer setting indicated a good seal. If we failed to obtain a constant value for P, we moved the micropipette to another spot on the surface of the myofiber or we replaced the micropipette. If neither of these was effective, we discarded the myofiber. We continuously checked the stability of P, except when the sarcolemma burst and P dropped slightly. We also periodically checked for the effectiveness of the seals by increasing and decreasing P. Typically, in myofibers in which the sarcolemma maintains its links to the underlying contractile apparatus, the height of a bleb (h) increases as P increases, and decreases as P decreases, with no change in the slope of the P–h curve (no hysteresis). Such curves were taken as additional evidence of good seals (Fig. 3).

The elastic model proposed by Rapoport (1972) analyzes the elastic behavior of the distortion and tension lines formed by myofibrils and the sarcolemma in response to suction pressures, P, applied over a small area as a bleb is formed. We followed a similar treatment to analyze our experimental results. P in dyne/cm^2, applied to the outer surface of the myofiber was calculated from $P = \rho g h_{man}$, where ρ is the density of the manometer fluid in g/cm^3, g = 981 cm/s^2 and h_{man} is the difference of levels in the manometer relative to P = 0 (Taylor 2005). We assumed that at equilibrium, when the height of the bleb becomes constant, the pressure inside the cell is the same as the suspending medium, whether this occurs before or after separation of the sarcolemma from the underlying structures. For each applied P, the height of the bleb formed inside the suction pipette, h, was measured in μm. At the SLs used for our studies, the diameters of the muscle fibers did not change noticeably as P increased and the bleb enlarged. As the total length of the myofiber does not change, the total cell volume therefore remains constant.

Once h was measured and P calculated, the average surface tension, γ in dyne/cm, was calculated, as follows:

$$P=\gamma\left(\frac{1}{r_1}+\frac{1}{r_2}\right) \quad (\mathrm{dyne/cm^2}) \quad (1)$$

where r_1 and r_2 are the radii of curvature of an asymmetric bent shell membrane. However, since the bleb is part of a symmetric sphere, then the centers of curvatures are the same. Therefore, $r_1 = r_2 = r$, the single radius of curvature (Rand 1964; Nelkon 1979; Pellicer et al. 2000). Thus

$$P=\frac{2\gamma}{r} \quad (\mathrm{dyne/cm^2}) \quad (2)$$

The radius, r, was computed from $r = d^2/8\,h + h/2$ (μm) from Pythagoras' Theorem (Dull 1941), where h and the pipette diameter d were measured. So substituting r in Eq. 2, it becomes:

$$P=\frac{2\gamma}{\left(\frac{d^2}{8h}+\frac{h}{2}\right)} \quad (\mathrm{dyne/cm^2}) \quad (3)$$

From the P–h curves the tension of the whole system, γ_{i+o} (dyne/cm), before separation of the sarcolemma, M_o, from the contractile apparatus, M_i, was calculated from Eq. 3. The tension of the isolated sarcolemma after separation from the contractile apparatus, γ_o (dyne/cm), was also estimated with Eq. 3, from the experimental data in the segment of the P–h curve after separation of the surface membrane from the myoplasm. In this condition, the myofibrils do not contribute to the tension of the surface membrane, as measured with the elastimeter. As a result, we were unable to measure the biomechanical characteristics of the myofibrils (see Rapoport 1972 for additional considerations).

The attachments between the peripheral myofibrils and the sarcolemma are assumed to be due to structures that link the myofibrils at costameres. The separation of the sarcolemma from the most superficial myofibrils takes place when high pressures (P) are applied to the surface membrane. Since the separation of myofibrils from the sarcolemma occurs without breaking either structure, we propose that the break takes place in the structures that link the myofibrils to the sarcolemma, i.e. the costameres and closely associated cytoplasmic structures. Therefore, the tension exerted by costameres and closely associated cytoplasmic structures (γ_c) is obtained by the subtraction of γ_o and γ_i from γ_{i+o}.

$$\gamma_{i+o}=\gamma_o+\gamma_i+\gamma_c \quad (\mathrm{dyne/cm})$$

Thus, $\gamma_c = \gamma_{i)o} - \gamma_o - \gamma_i$ (dyne=cm)

Because $\gamma_i = 0$ when the sarcolemma has separated from the contractile apparatus, it does not contribute to γ_c. Therefore,

$$\gamma_c=\gamma_{i+o}-\gamma_o \quad (\mathrm{dyne/cm}) \quad (4)$$

The myofibrils, costameres and associated structures, and sarcolemma were considered as three different spring elements, each with its own elastic properties. The sarcolemma and myofibrils act as springs in parallel, linked at right angles by the spring-like elements at costameres. At equilibrium muscle length (2 μm/SL), the springs are not stretched but when the fiber is stretched to >2 μm/SL, the tension of each spring increases as a function of the SL.

The force, F, in dynes applied to the membrane at a given suction pressure is estimated from:

$$P=\frac{F}{A} \quad (\mathrm{dyne/cm^2}) \quad (5)$$

Since the radius, r, of the pipette is always the same, we can estimate the area, A, of the segment of the spherical shell of the sarcolemma inside the pipette at different Ps. Therefore, F = PA (dyne), where A in cm^2 is the area of the segment of the spherical shell bleb to which the force is applied. A can be calculated from $A = 2\pi rh$, where r and h are defined as above.

The stiffness or spring constant (k) is related to the ability of the cell to resist deformation when subjected to load (Leckie and Dal Bello 2009). This also represents the elasticity of the material under study. Specifically, the more elastic a material is, the less it is deformed by a given force. Therefore, the less elastic the material, the more compliant it is. The breaking point is the maximum load that a system can support before a complete failure of the structure of the material in question. k was estimated from F = kh (dyne) (Taylor 2005). Therefore,

$$k=\frac{F}{h} \quad (\mathrm{dyne/cm}) \quad (6)$$

Other authors have also calculated cell stiffness (k), by measuring the applied force (F) and the displacement it caused on the cell membrane (Petersen et al. 1982; Pasternak et al. 1995; Pasternak and Elson 1985; Wojcikiewicz and Zhang 2004).

As surface tension is inversely proportional to temperature (Bull 1964), we performed our experiments at a constant temperature of 8.0 ± 0.5°C. The same fiber could be used for up to 4 h before showing signs of deterioration (e.g., spontaneous membrane blebbing, localized swelling, spontaneous localized changes of SL, or lack of reproducibility of the data obtained from nearby regions of the same fiber).

Data acquisition

Images were obtained with a digital camera (Nikon D-70 NY, USA) with an effective resolution of 6.1 Mpixels. The camera was placed above the microscope with an external device independent of the microscope and linked instrumentation, to avoid transmission of vibrations. Several images of the bleb were taken before and after the time at which the height of the bleb was stable, but for the measurements described here only the last ones were examined and used for quantification. Recoverable deformations in membranes have been observed and studied since the beginning of microscopic observations of cell morphology (Rand 1964; Evans and Hochmuth 1976). In our case after P was applied, it took some time for the bleb to reach a stable height, suggesting viscoelastic behavior (Rapoport 1972; Garcia-Pelagio et al. 2008), i.e., behavior resembling that of an elastic solid on short time-scales and of a viscous fluid on long time-scales (Boal 2006). The photographs were transferred to a PC with Adobe Photoshop™ 7.0.1. The measurements of the height, h, of the bleb formed inside the suction pipette were analyzed with Image J (NIH, Bethesda,

MD). A microphotograph of a stage micrometer scale, calibrated in microns, was also taken and transferred to the PC, to determine the relationship between pixel number and μm.

Statistics

Data for tension, pressure and stiffness were analyzed with a 2-way analysis of variance (ANOVA) with a post hoc analysis (Kruskal–Wallis). Values of $P < 0.05$ were considered statistically significant. All results are reported as mean ± standard deviation (SD). We also report the statistical population variance (V) of tension and pressure measurements, which indicates the degree of dispersion or scattering of the experimental data.

Source of materials

Unless indicated, all chemicals were purchased from Sigma-Aldrich (St. Louis, MO).

Results

Elastimetry in mouse myofibers

The elastic properties of the sarcolemma and the strength of its connections to the underlying contractile apparatus were assessed by elastimetry. The method uses suction pressure (P), applied over a small sarcolemmal area (approximately 250 μm^2) through a suction pipette. With myofibers at an average SL of 2 μm or less, application of negative pressure to the surface by a large bore suction pipette, with a diameter approaching that of the myofiber itself, the sarcolemma and nearby myoplasm were sucked into the pipette, without a significant change in surface tension. This also occurred at SLs >2 μm when we used large bore pipettes. However, at SLs above 2 μm and with micropipettes with tip diameters of 0.50–0.66 myofiber diameter, this did not occur; instead, the sarcolemma stretched and surface tension (γ) increased. These results are consistent with previous studies of frog myofibers (Rapoport 1972), but as the diameters of murine myofibers are half or less of frog myofibers, our experiments required much larger suction pressures, which we achieved with a different set of manometers (see “Materials and methods” section). At SLs < 3 μm the sarcolemma has invaginations and caveolae (Dulhunty and Franzini-Armstrong 1975). During formation of blebs at short SLs, caveolae are unfolded as the suction pressure, P, is increased, raising the possibility that, at short SLs, the calculation of the surface tension may be misleading. We therefore also routinely obtained P–h curves at SLs >3.5 μm, where further contributions of caveolae are likely to be minimal (Dulhunty and Franzini-Armstrong 1975). We ensured that the values we determined were at equilibrium, when the bleb no longer underwent changes in h.

When we used small bore micropipettes to study myofibers stretched to SLs >3.5 μm, the application of suction pressure to the surface of the fiber induced the formation of a bleb of variable height, h, which was a function of both P and SL (Fig. 2a–j). At low negative pressures, the sarcolemma and the associated contractile apparatus underlying it were drawn into the pipette together (Fig. 2a). The movement of contractile apparatus into pipette was small compared to the fiber diameter, which minimized changes in volume. Upon relaxation of P, h decreased and the bleb returned to its initial height. As the suction pressure increased, h increased, until at large negative pressures the sarcolemma (Fig. 2b; indicated by M_o)

separated from the contractile apparatus, which remained distended (Fig. 2b; indicated by M_i), even when the pressure was relieved. Further increases in P produced further increases in h but had only minimal effects on nearby myofibrils (not shown, but see Rapoport 1972).

We obtained a series of microphotographs of sarcolemmal blebs that were formed with progressively increasing suction pressures in myofibers isolated from the EDL muscles of *WT* (Fig. 2c–f) and dystrophin-null, *mdx* (Fig. 2g–j) mice. We generated vertical pressure–displacement (P–h) curves from all fibers, and analyzed them to determine the blebbing behavior of the sarcolemma and nearby myofibrils as a function of P. We did not observe significant changes in the SL or nearby myofibrils that contributed to the formation of the bleb and its growth as P was gradually increased, suggesting that the sarcolemma and nearby myofibrils retained their structural relationship (Fig. 2). The relationship of the myofibrils to the SL did, however, change markedly when P was increased further, leading to the separation of these structures (see below).

Vertical bleb displacement, h, is a function of the suction pressure, P

The experimental pressure–displacement (P–h) curve for *WT* muscle showed three distinct segments (Fig. 3a). In the first, obtained at low suction pressures (Fig. 3a, points 2–16), the sarcolemma remained closely associated with nearby myofibrils under the bleb. The P–h relationship in this segment was reversible (Fig. 3a, points 8–10 and 14–16), with no hysteresis when P was reduced. Consistent with this, morphological observations indicated that the system formed by the contractile apparatus, costameres, and the sarcolemma remained intact.

In the next portion of the P–h curve (Fig. 3a, points 17–19), measured at higher suction pressures, the slope decreased. This decrease in slope was accompanied by the physical separation of the sarcolemma from the myofibrils (Fig. 3a, point S). Thus, in this range the sarcolemma distended more for the same increase in pressure, presumably because it was not restrained by links to contractile structures.

The third segment of the curve (Fig. 3a, points 19–23), obtained by reducing P after separation of the sarcolemma from underlying myofibrils, resulted in different values of h at a given value of P than before separation. Larger changes in h occurred for the same changes in P, than in the rising portion of the curve. This hysteresis in the P–h curve indicates that the biomechanical system is different before and after separation of the sarcolemma.

We calculated the surface tension, γ, from the slope of the P–h curve (see “Elastimetry” section, in Materials and methods). For single, isolated myofibers from *WT* mice, the three segments of the curve yielded 3 distinct slopes, for the intact system, including the elastic constants (k_{i+o}) of myofibrils, costameres and sarcolemma, for the sarcolemma immediately after separation, and for the final segment, which reflects the elastic properties of the isolated sarcolemma (k_o). In wild type muscle, the elastic constant of the sarcolemma alone, k_o, was ~80% that of the intact system, k_{i+o} (Table 1). As the sarcolemma and myofibrils remain intact after separation, the links between them, established in part at costameres, are the weakest structures in the system.

We used the same methods to determine the P–h relationship in myofibers isolated from *mdx* mice. Although the shapes of the curves were similar, the values we obtained for the pressure at which separation occurred, P_{sep}, for surface tension, γ, and for k_{i+o} and k_o, were consistently ~2-fold lower than in *WT* muscle (Table 1), suggesting that the stiffness of the system encompassing the sarcolemma, costameres and nearby myofibrils, and the strength of the connections between the sarcolemma and myofibrils, are significantly compromised when dystrophin is absent (Fig. 4a). In the absence of dystrophin, the sarcolemma is more easily distended at a given pressure, and the slopes of each phase of the P–h curves are greater in the *WT* than in the *mdx* (Fig. 4b).

The effect of SL

The slopes of the rising portions of the P–h curves showed a strong dependence on SL at pressures at which the sarcolemma remains attached to the underlying myofibrils. In particular, higher pressures were required to produce the same increase in h (Fig. 3b, solid lines). This suggests that the contractile apparatus contributes significantly to the stiffness of the sarcolemma in the intact system. This was not the case after sarcolemmal separation, however; these descending portions of the P–h curve showed little change with SL, indicating that the contractile apparatus had no influence on the elasticity of the isolated sarcolemma.

P_{sep} was also a function of SL, with higher pressures needed to cause separation as SL increased (Figs. 3b, 4a). The change in P_{sep} was greatest at SLs from 3.6 to 4.3 μm. Changes at SLs between 2.9 and 3.4 μm (data not shown) were not statistically significant.

Consistent with the lower stiffness measured for the surface membrane and nearby myofibrils in *mdx* myofibrils, we found that P_{sep} was reduced by 2-fold at SLs between 3.6 and 4.3 μm (Fig. 4a; Table 1; $P > 0.05$). These results suggest that the sarcolemmal links to the myofibrils fibers are significantly weakened in *mdx* muscle.

Elastic behavior

The sarcolemma and nearby contractile apparatus can be modeled as an elastic body composed of three main elements, sarcolemma, costameres and myoplasm, each with its own elastic characteristics that together generate the elastic properties of the whole system. We first characterized the elastic properties, tension and stiffness, of the whole system and those of the costameres and sarcolemma, in *WT* mice and then compared the results with those obtained with *mdx* mice.

Using the Young–Laplace equation (Eq. 2) and the data in our P–h curves, we computed the total tension of the system, γ_{i+o} (Fig. 5a), the sarcolemmal tension, γ_o (Fig. 5b), and the maximal tension sustained by the costameres and their links to the myofibrils, γ_c (Fig. 5c). The value for γ_c was obtained by subtracting γ_o from γ_{i+o} (Table 1). The total tension sustained by the whole system and by the isolated sarcolemma in *WT* myofibers was significantly larger than for *mdx* myofibers at all SLs examined ($P < 0.05$). As γ_{i+o} increased for *WT* but not for *mdx* at SLs >3.6 μm, these differences become greater. Similarly, γ_o for *WT* was consistently greater than for *mdx*, with the differences reaching significance ($P <$

0.05) at SLs between 3.8 and 4.3 μm. The calculated values for γ_c, obtained by subtracting γ_o from γ_{i+o}, were increased significantly at SLs of ≥3.4 μm, with differences of ~5-fold at longer SLs (Fig. 5c; Table 1).

We also examined the variance, V, of our measurements to assess the variability. The V of measurements of γ were generally greater for *WT* than for *mdx* (Table 1). We suggest that dystrophin is an elastic element, linking the sarcolemma to the contractile myofibers, which stretches as SL is increased.

We computed the stiffness (k) of the system and its elements as described above (Eq. 6) and the slope of the Force–displacement (F–h) curve (Fig. 5d, e). These values, too, decreased significantly in *mdx* myofibers compared to *WT* ($P < 0.01$; Table 1).

$P_{bursting}$ of the sarcolemma

Further increases of suction pressure, P, after separation of the sarcolemma from nearby myofibrils, eventually caused the membrane bleb to burst (Fig. 6a, b). The pressure at which sarcolemmal bursting occurred, $P_{bursting}$, was independent of SL (Fig. 6c), as expected, but was consistently higher in *WT* than in *mdx* myofibers (Fig. 6a; Table 1; $P < 0.01$). This supports the idea that dystrophin stabilizes the sarcolemmal membrane, independent of its possible contributions at costameres and their links to nearby contractile structures.

Discussion

We used a modified elastimeter to measure the membrane bending elasticity of the sarcolemma of mammalian myofibers. A major advantage of this method is that the geometry and tension of the membrane is well controlled during the experimental measurements, which allowed us to quantify the changes in membrane area as a function of suction pressure (Evans and Hochmuth 1976; Needham and Hochmuth 1992), as well as related changes. In adapting a method originally designed for frog myofibers (Rapoport 1972), which are significantly larger than mammalian myofibers, we had to use micropipettes of smaller diameter, which in turn required manometers that could operate at much higher pressures. Our methods have allowed us to study several biomechanical properties of the surface of mature fibers of the murine EDL muscle, but they can easily be modified to study cells with very different surface rigidities. Given the high pressures needed to obtain detachment and bursting, other quantitative methods, including optical tweezers and atomic force microscopy, would likely be ineffective. Our results indicate that the elasticity and stability of the sarcolemma and the strength of its links to nearby myofibrils are severely compromised in the absence of dystrophin.

Our experiments are the first to determine the biomechanical properties of the sarcolemmal membrane and the links it establishes via costameres to nearby myofibrils. We achieved this by studying the properties of the sarcolemma while it remained attached to the underlying contractile apparatus, and after it separated from contractile structures at higher applied pressures. The properties of the isolated sarcolemma, obtained after detachment at higher pressures, were independent of SL. Comparison of the two conditions suggest that ~80% of the stiffness of the muscle cell surface is attributable to the sarcolemma and closely

associated structures, including the membrane-associated cytoskeleton and the basement membrane. Nevertheless, the stiffness of the myofiber surface, with the sarcolemma connected to underlying contractile structures, is influenced by the latter, as increases in SL result in significant increases in stiffness (Table 1; Fig. 5d, e). This is consistent with the idea that much of the contractile force in skeletal muscle is transduced along lateral pathways of force transmission (e.g., Street 1983; Bloch and Gonzalez-Serratos 2003).

Our studies are also the first to assess the role of dystrophin in determining the biomechanical properties of the sarcolemma linked to nearby myofibrils, and of the sarcolemma immediately after detachment from contractile elements. Our measurements demonstrate that the absence of dystrophin in the EDL muscles of *mdx* mice decreases both the pressure needed to detach the sarcolemma from superficial myofibrils, P_{sep}, and the pressure needed to burst the sarcolemma, $P_{bursting}$. Our results suggest that the sarcolemma of muscle fibers lacking dystrophin is more compliant and less stable than control muscles. The role of dystrophin on isolated segments of the sarcolemma agrees with earlier studies that showed that dystrophin associates with the sarcolemma when it is mechanically pealed away from the contractile apparatus (Rybakova et al. 2000). We cannot rule out the possibility that the absence of dystrophin leads to other, secondary changes at the sarcolemma or the extracellular matrix, including the basal lamina, collagen fibrils, or other proteins of the reticular lamina that may affect these properties. Nevertheless, our results suggest that dystrophin stabilizes the sarcolemma and participates in the links between that membrane and the contractile apparatus, anchored at costameres.

We were able to deduce some of the biomechanical properties of costameres by comparing the properties of the sarcolemma in two configurations, attached and detached from the underlying contractile apparatus. Our results suggest that costameres, and the links between the sarcolemma and the contractile apparatus that they anchor, are significantly weaker than the sarcolemma itself, contributing only ~20% of the stiffness seen in the intact biomechanical system. As dystrophin is normally concentrated at costameres (Porter et al. 1992; Straub et al. 1991; Ervasti 2003) it is not surprising that the strength of these links is compromised in the *mdx* mouse. Several proteins are likely to interact with dystrophin to establish these links, including γ-actin, intermediate filaments composed of desmin and of keratins, as well as other proteins (Rybakova et al. 2000; O'Neill et al. 2002; Stone et al. 2007). Similar studies of muscles lacking each of these proteins should reveal how they contribute to the stability of costameres and the connectivity of the sarcolemma and contractile elements.

Analysis of the statistical variance, V, of our values for P_{sep} offers additional insights into the nature of the costameres and their links to the contractile apparatus. The variance of P_{sep} with SL is considerably lower for *mdx* than *WT* (100 ± 10 for *WT*, 9 ± 3 for *mdx*). This indicates that if an important elastic element, such as dystrophin, is missing, the system becomes more compliant. When the surface membrane is attached to underlying myofibrils via costameres, stretching the links will produce a larger change in force than when these links are broken, and this in turn will produce a higher variance.

Comparison of our results with those obtained in the semitendinosus muscles of *Rana pipiens* suggests that the sarcolemma of the latter is weaker than that of the mouse EDL muscle. At SLs of 4 μm, Rapoport (1972) measured an average $\gamma = 45$ dyne/cm for the frog semitendinosus. Our values are 3–5-fold higher. Similar differences are also found at shorter SLs. Although some of the difference may be due to temperature (22°C, compared to 8°C, used here), which affects surface tension (Bull 1964), studies of single EDL fibers at different temperatures indicate that the Q_{10} for total surface tension is ~3.9 (not shown), which is not sufficient to account for the different values for γ in frog and mouse muscles. The higher total surface tension of the EDL myofibers may be due to the presence in mammalian striated muscle of costameres that link superficial myofibrils to the sarcolemma at the levels of the Z-disks and M-bands, and that may also include longitudinal elements. By contrast, amphibian semitendinosus myofibers have costameres only at the level of Z-disks (Street 1983; Gonzalez-Serratos, unpublished results). The presence of more links in EDL muscles would produce stiffer surface membranes and larger surface tensions. As a substantial percentage of active force is transmitted laterally through the costameres to the tendons (Street 1983; Bloch and Gonzalez-Serratos 2003), the higher density of costameres in mammalian muscle may explain why a single murine flexor digitorum brevis myofiber generates a specific force of 362 kPa (Allen et al. 2008), compared to 275 kPa for an isolated amphibian muscle cell (Gordon et al. 1966), when both are measured at optimal SL.

The images of Williams and Bloch (1999a, b) suggest that costameres cover approximately half of the surface membrane of fast twitch muscle fibers. At an average SL of 2.9 or 3.6 μm, the pressure exerted on sarcolemma just before it separates from the underlying contractile apparatus is approximately 2.6×10^9 Pa. If this pressure is distributed evenly across all domains of the costameres, then the pressure exerted on the links between the contractile apparatus and the sarcolemma, present at costameres, would be approximately twice this value, or approximately 5.2×10^9 Pa. We previously estimated that during a maximal tetanic contraction the lateral pressure exerted on the sarcolemma is approximately 6×10^5 Pa (Bloch and Gonzalez-Serratos 2003). This indicate that the costameres have a safety factor of several orders of magnitude that would make it highly unlikely for them to break during normal muscle function or even during a maximal lengthening contraction.

Even in their weakened state, in the *mdx* muscle, costameres should be more than strong enough to withstand damage caused by contractile activity. Thus, damage to the sarcolemma that occurs during forceful contractions, in *mdx* as well as in wild type muscle, is likely to arise from areas between the costameres, the “intercostameric regions”, which lack many of the structural proteins that reinforce the costameres themselves (Williams and Bloch 1999b). The fact that dystrophin and its associated proteins are present in the intercostameric regions of wild type muscle, but not *mdx* muscle (Williams and Bloch 1999b), may therefore account for the greater susceptibility of the latter to damage linked to contractile activity.

Other authors have used aspiration pipettes to measure cell surface tension (γ) in a variety of cells. In neutrophils, Needham and Hochmuth (1992) extrapolated the tension in a resting membrane at room temperature and obtained a $\gamma = 2.4 \times 10^{-2}$ dyne/cm, similar to the value of 2.7×10^{-2} dyne/cm reported by Tsai et al. (1993). In granulocytes, Evans and Yeung (1989) found $\gamma = 3.5 \times 10^{-2}$ dyne/cm for granulocytes while Trans-Son-Tay et al. (1991)

reported a value of 2.4×10^{-2} dyne/cm. In chick embryo fibroblasts, Thoumine et al. (1999) and Rand (1964) found a maximum $\gamma = 2.4$ dyne/cm, while Waugh and Evans (1979) reported $\gamma = 6.6$ dyne/cm. Hutter et al. (1991) measured the tension of isolated sarcolemmal vesicles alone ("sarcoballs") obtained from semimembranosus muscles by exposing excised muscles to KCl and collagenase at room temperature. They reported an average bursting tension of 6 dyne/cm in sarcoballs from myofibers of *WT* mice and of 5.2 dyne/cm in sarcoballs of myofibers from *mdx* mice. The difference is smaller than the one we found here. This smaller difference is probably due to the fact that sarcoballs are spheres composed of the sarcolemma alone, and that many peripheral membrane proteins, such as dystrophin, may be shed from the cytoplasmic surface of the sarcolemma as sarcoballs form.

Using a different approach, Pasternak et al. (1995) reported that the stiffness of myotubes prepared from *mdx* mice was 3.4 dyne/cm, several fold lower than the value of 12.3 dyne/cm that they measure for controls. As myotubes lack an organized contractile apparatus and do not readily form costameres (Bloch, unpublished results; but see Quach and Rando 2006), the fact that they were considerably less stiff than myofibers (our values for stiffness are considerably higher) is not surprising. Their use of cells in culture prevented Pasternak et al. (1995) from controlling SL, and the glass rods they employed to indent the surface membranes also did not allow them to control for the contribution of caveolae to the membrane as it deformed. Both of these factors also contribute to the lower values they obtained. The higher values that we report for the surface membrane of intact skeletal muscle fibers are likely due to presence of an extensive membrane-associated cytoskeleton that underlies the sarcolemma and that links it to contractile structures (Porter et al. 1992; Williams and Bloch 1999a; Hutter et al. 1991; Na et al. 2009).

Bobet et al. (1998) and Wolff et al. (2006) reported that there were no differences in the passive mechanical or active contractile properties of whole EDL muscles from *mdx* and control mice. It is difficult to compare results obtained with whole muscles to single isolated myofibers, because of the many additional elastic elements present in the former, some of which increase in *mdx* muscle (Goldspink et al. 1994). As we find that the surface of *mdx* myofibers is more compliant than controls, the changes in the extracellular matrix (and possibly other structures lying between myofibers) in *mdx* mice are likely to compensate for this increased compliance in whole muscles. The fact that the stiffness of the surface of *mdx* myofibers is ~100 fold greater than that of *WT* or *mdx* myotubes is consistent with the idea that, despite its importance for the health of muscle and the stability of the sarcolemma, factors others than dystrophin play important roles in determining the biomechanical properties of the muscle cell surface. The absence of dystrophin results in a decrease in the lateral transmission of passive force, linked to changes in the properties of costameres. The decrease in costameric strength and stiffness in *mdx* myofibers could also lead to a decrease in the lateral transmission of active force during contraction (Street 1983; Bloch and Gonzalez-Serratos 2003). We are currently studying the roles of several other proteins that are enriched at costameres, with the goal of developing a comprehensive physical model of these structures and how they contribute to lateral force transmission.

Acknowledgments

This research was partially supported by grants to R. J. Bloch from the National Institute of Heath (5R01AR055928) and the Muscular Dystrophy Association. K. P. García-Pelagio was supported during the Ph. D. program (Doctorado en Ciencias Biomédicas, Universidad Nacional Autónoma de México) by a scholarship from Consejo Nacional de Ciencia y Tecnología.

References

Allen DG, Lamb GD, Westerblad H. Skeletal muscle fatigue: cellular mechanisms. Physiol Rev. 2008; 88:287–332. [PubMed: 18195089]

Anastasi G, Cutroneo G, Santoro G, Arco A, Rizzo G, Bramanti P, Rinaldi C, Sidoti A, Amato A, Favaloro A. Costameric proteins in human skeletal muscle during muscular inactivity. J Anat. 2008; 213(3):284–295. [PubMed: 18537849]

Ayalon G, Davis J, Scotland P, Bennett V. An ankyrin-based mechanism for functional organization of dystrophin and dystroglycan. Cell. 2008; 135(7):1189–1200. [PubMed: 19109891]

Barton E. Impact of Sarcoglycan complex on mechanical signal transduction in murine skeletal muscle. Am J Physiol Cell Physiol. 2006; 290(2):C411–C419. [PubMed: 16162659]

Beedle A, Nienaber P, Campbell K. Fukutin-related protein associates with the sarcolemmal dystrophin–glycoprotein complex. J Biol Chem. 2007; 282(23):16713–16717. [PubMed: 17452335]

Bhosle R, Michele D, Campbell K, Li Z, Robson R. Interactions of intermediate filament protein synemin with dystrophin and utrophin. Biochem Biophys Res Commun. 2006; 346(3):768–777. [PubMed: 16777071]

Blaauw B, Mammucari C, Toniolo L, Agatea L, Abraham R, Sandri M, Reggiani C, Schaffino S. Akt activation prevents the force drop induced by eccentric contractions in dystrophin-deficient skeletal muscle. Hum Mol Genet. 2008; 17(23):3686–3696. [PubMed: 18753145]

Blaauw B, Agate L, Toniolo L, Canato M, Quarta M, Dyar K, Danieli-Betto D, Betto R, Schiaffino S, Reggiani C. Eccentric contractions lead to myofibrillar dysfunction in muscular dystrophy. J Appl Physiol. 2010; 108(1):105–111. [PubMed: 19910334]

Bloch R, Gonzalez-Serratos H. Lateral force transmission across costameres in skeletal muscle. Exerc Sport Sci Rev. 2003; 31(2):73–78. [PubMed: 12715970]

Bloch R, Capetanaki Y, O'Neill A, Reed P, Williams MW, Resneck W, Porter N, Ursitti J. Costameres: repeating structures at the sarcolemma of skeletal muscle. Clin Orthop Relat Res. 2002; 403S:S203–S210. [PubMed: 12394470]

Boal, D. Mechanics of the cell. Cambridge University Press; Cambridge: 2006.

Bobet J, Mooney RF, Gordon T. Force and stiffness of old dystrophic (mdx) mouse skeletal muscles. Muscle Nerve. 1998; 21(4):536–539. [PubMed: 9533791]

Brenman J, Chao D, Xia H, Aldape K, Bredt D. Nitric oxide synthase complexed with dystrophin and absent from skeletal muscles sarcolemma in Duchenne muscular dystrophy. Cell. 1995; 82(5): 743–752. [PubMed: 7545544]

Bull, H. An introduction to physical biochemistry. Davis Co; Philadelphia: 1964.

Campbell K, Stull T. Skeletal muscle basement membrane–sarcolemma–cytoskeleton interaction minireview series. J Biol Chem. 2003; 278(15):12599–12600. [PubMed: 12556456]

Caputo C, Bolaños P. Fluo-3 signals associated with potassium contractures in single amphibian muscle fibers. J Physiol. 1994; 481:119–128. [PubMed: 7853234]

Claffin D, Brooks S. Direct observation of failing fibers in muscles of dystrophic mice provides mechanistic insight into muscular dystrophy. Am J Physiol Cell Physiol. 2008; 294:C651–C658. [PubMed: 18171725]

Dmytrenko G, Pumplin D, Bloch R. Dystrophin in membrane skeletal network: localization and comparison to other proteins. J Neurosci. 1993; 13(2):547–558. [PubMed: 8426227]

Dulhunty AF, Franzini-Armstrong C. The relative contribution of the folds and caveolae to the surface membrane of frog skeletal muscle fibers at different sarcomere length. J Physiol. 1975; 250:513–539. [PubMed: 1080806]

Dull, RW. Mathematics for engineers. McGraw-Hill Book Company; New York: 1941.

Ehmer S, Herrmann H, Bittner R, Voit T. Spatial distribution of beta-spectrin in normal and dystrophic human skeletal muscle. Acta Neuropathol. 1997; 94(3):240–246. [PubMed: 9292693]

Ervasti J. Costameres: the Achilles' heel of herculean muscle. J Biol Chem. 2003; 278(16):13591–13594. [PubMed: 12556452]

Ervasti J. Dystrophin, its interactions with other proteins, and implications for muscular dystrophy. Biochem Biophys Acta. 2007; 1772(2):108–117. [PubMed: 16829057]

Ervasti J, Campbell K. Membrane organization of the dystrophin–glycoprotein complex. Cell. 1991; 66(6):1121–1131. [PubMed: 1913804]

Ervasti J, Campbell K. A role for the dystrophin–glycoprotein complex as a transmembrane linker between laminin and actin. J Cell Biol. 1993; 122:809–823. [PubMed: 8349731]

Evans E, Hochmuth M. Membrane viscoelasticity. Biophys J. 1976; 16(1):1–11. [PubMed: 1244886]

Evans E, Yeung A. Apparent viscosity and cortical tension of blood granulocytes determined by micropipette aspiration. Biophys J. 1989; 56:151–160. [PubMed: 2752085]

Fonbrune, P. Technique de Micromanipulation. Massonn et Cie; Paris: 1949.

Garcia-Pelagio K, Bloch R, Ortega A, Gonzalez-Serratos H. Elastic properties of the sarcolemma–costamere complex of muscle cells in normal mice. AIP Conf Proc. 2006; 854:51–53.

Garcia-Pelagio K, Bloch R, Ortega A, Gonzalez-Serratos H. Passive viscoelastic properties of costameres in EDL muscle in normal and dystrophin null mice. AIP Conf Proc. 2008; 1032:268–271.

Goldspink G, Fernandes K, Williams PE, Wells DJ. Age-related changes in collagen gene expression in the muscles of mdx dystrophic and normal mice. Neuromuscul Disord. 1994; 4(3):183–191. [PubMed: 7919967]

Gonzalez-Serratos H. Inward spread of activation in vertebrate muscle fibres. J Physiol. 1971; 212(3):777–799. [PubMed: 5557071]

Gordon AM, Huxley AF, Julian FJ. The variation in isometric tension with sarcomere length in vertebrate muscle fibers. J Physiol. 1966; 184:170–192. [PubMed: 5921536]

Hochmuth M. Micropipette aspiration of living cells. J Biomech. 2000; 33:15–22. [PubMed: 10609514]

Hoffman EP, Brown R, Kunkel L. Dystrophin: the protein product of the Duchenne muscular dystrophy locus. Cell. 1987; 51:919–928. [PubMed: 3319190]

Hutter OF, Burton FL, Bovell DL. Mechanical properties of normal and mdx mouse sarcolemma: bearing on function of dystrophin. J Muscle Res Cell Motil. 1991; 12:585–589. [PubMed: 1791198]

Lapidos K, Kakkar R, McNally M. The dystrophin glycoprotein complex: signaling strength and integrity for the sarcolemma. Circ Res. 2004; 94:1023–1031. [PubMed: 15117830]

Leckie, FA.; Dal Bello, DJ. Strength and stiffness of engineering systems. Springer; New York: 2009.

Minetti C, Cordone G, Beltrame F, Bado M, Bonilla E. Disorganization of dystrophin costameric lattice in Becker muscular dystrophy. Muscle Nerve. 1998; 21(2):211–216. [PubMed: 9466596]

Mitchison JM. The thickness of the sea urchin fertilization membrane. Exp Cell Res. 1953; 5(2):536–538. [PubMed: 13117023]

Na S, Chowdhury F, Tay B, Ouyang M, Gregor M, Wang Y, Wiche G, Wang N. Plectin contributes to mechanical properties of living cells. Am J Physiol Cell Physiol. 2009; 296(4):C868–C877. [PubMed: 19244477]

Needham D, Hochmuth M. A sensitive measure of surface stress in the resting neutrophil. Biophys J. 1992; 61(6):1664–1670. [PubMed: 1617145]

Nelkon, M. Scholarship physics. Hienemann Educational Publishers; London: 1979.

Nigro V, Piluso G, Belsito A, Politano L, et al. Identification of a novel sarcoglycan gene at 5q33 encoding a sarcolemmal 35 kDa glycoprotein. Hum Mol Genet. 1996; 5(8):1179–1186. [PubMed: 8842738]

Nowak K, Davies K. Duchenne muscular dystrophy and dystrophin: pathogenesis and opportunities for treatment. EMBO Rep. 2004; 5:872–876. [PubMed: 15470384]

O'Neill A, Williams MW, Resneck W, Milner D, Capetanaki Y, Bloch RJ. Sarcolemmal organization in skeletal muscle lacking desmin: evidence for cytokeratins associated with membrane skeleton at costameres. Mol Biol Cell. 2002; 13:2347–2359. [PubMed: 12134074]

Oak SA, Zhou YW, Jarrett HW. Skeletal muscle signaling pathway through the dystrophin glycoprotein complex and Rac1. J Biol Chem. 2003; 278(41):39287–39295. [PubMed: 12885773]

Ohlendieck K, Ervasti J, Snook J, Campbell K. Dystrophin–glycoprotein complex is highly enriched in isolated skeletal muscle sarcolemma. J Cell Biol. 1991; 112:135–148. [PubMed: 1986002]

Ozawa E. From dystrophinopathy to sarcoglycanopathy: evolution of a concept of muscular dystrophy. Muscle Nerve. 1998; 21:421–438. [PubMed: 9533777]

Pasternak C, Elson E. Lymphocyte mechanical response triggered by cross-linking surface receptors. J Cell Biol. 1985; 100:860–872. [PubMed: 4038710]

Pasternak C, Wong S, Elson E. Mechanical function of dystrophin in muscle cells. J Cell Biol. 1995; 128(3):355–361. [PubMed: 7844149]

Pellicer J, García-Morales V, Hernández MJ. On the demonstration of the Young–Laplace equation in introductory physics courses. Phys Educ. 2000; 35(2):126–129.

Petersen N, McConnaughey W, Elson E. Dependence of locally measured cellular deformability on position on the cell, temperature, and cytochalasin B. Proc Natl Acad Sci USA. 1982; 79:5327–5331. [PubMed: 6957866]

Petrof B, Shrager J, Stedman H, Kelly A, Sweeney L. Dystrophin protect the sarcolemma from stresses developed during muscle contraction. Proc Natl Acad Sci USA. 1993; 90:3710–3714. [PubMed: 8475120]

Porter G, Dmytrenko G, Winkelmann J, Bloch R. Dystrophin colocalizes with beta-spectrin in distinct subsarcolemmal domains in mammalian skeletal muscle. J Cell Biol. 1992; 117(5):997–1005. [PubMed: 1577872]

Quach NL, Rando TA. Focal adhesion kinase is essential for costamerogenesis in cultured skeletal muscle cells. Dev Biol. 2006; 293:38–52. [PubMed: 16533505]

Rand RP. Mechanical properties of the red cell membrane. Biophys J. 1964; 4:303–316. [PubMed: 14197789]

Rapoport S. Mechanical properties of the sarcolemma and myoplasm in frog muscle as a function of sarcomere length. J Gen Physiol. 1972; 59:559–585. [PubMed: 4537306]

Reed P, Bloch RJ. Postnatal changes in sarcolemmal organization in mdx mouse. Neuromuscul Disord. 2005; 15(8):552–561. [PubMed: 16051092]

Rybakova I, Patel J, Ervasti J. The dystrophin complex forms a mechanically strong link between the sarcolemma and costameric actin. J Cell Biol. 2000; 150(5):1209–1214. [PubMed: 10974007]

Shah S, Davis J, Weisleder N, Kostavassili I, McCulloch A, Raltson E, Capetanaki Y, Lieber R. Structural and functional roles of desmin in mouse skeletal muscle during passive deformation. Biophys J. 2004; 86:2993–3008. [PubMed: 15111414]

Stone MR, O'Neill A, Lovering R, Strong J, Resneck WG, Reed PW, Toivola D, Ursitti J, Omary BM, Bloch RJ. Absence of keratin 19 in mice causes skeletal myopathy with mitochondrial and sarcolemmal reorganization. J Cell Sci. 2007; 120(22):3999–4008. [PubMed: 17971417]

Straub V, Bittner R, Leger J, Voit T. Direct visualization of the dystrophin network on skeletal muscle fiber membrane. J Cell Biol. 1991; 119(5):1183–1191. [PubMed: 1447296]

Street SE. Lateral transmission of tension in frog myofibers: a myofibrillar network and transverse cytoskeletal connections are possible transmitters. J Cell Physiol. 1983; 114:346–364. [PubMed: 6601109]

Taylor, R. Classical mechanics. University Science Books; Sausalito: 2005.

Thoumine O, Cardoso O, Meister JJ. Changes in the mechanical properties of fibroblasts during spreading: a micromanipulation study. Eur Biophys J. 1999; 28(3):222–234. [PubMed: 10192936]

Trans-Son-Tay R, Needham D, Yeung A, Hochmuth M. Time-dependent recovery of passive neutrophils after large deformation. Biophys J. 1991; 60(4):856–866. [PubMed: 1742456]

Tsai M, Frank R, Waugh R. Passive mechanical behavior of human neutrophils: power law fluid. Biophys J. 1993; 65:2078–2088. [PubMed: 8298037]

Ursitti JA, Lee PC, Resneck WG, McNally MM, Bowman AL, O'Neill A, Stone MR, Bloch RJ. Cloning and characterization of cytokeratins 8 and 19 in adult rat striated muscle. Interaction with the dystrophin glycoprotein complex. J Biol Chem. 2004; 279(40):41830–41838. [PubMed: 15247274]

Waugh E, Evans E. Thermoelasticity of red blood cell membrane. Biophys J. 1979; 26:115–132. [PubMed: 262408]

Wieneke S, Stehle R, Li Z, Jockusch H. Generation of tension by skinned fibers and intact skeletal muscles from desmin-deficient mice. Biochem Biophys Res Commun. 2000; 278:419–425. [PubMed: 11097852]

Williams MW, Bloch RJ. Extensive but coordinate reorganization of the membrane skeleton in myofibers of dystrophic (mdx) mice. J Cell Biol. 1999a; 144:1259–1270. [PubMed: 10087268]

Williams MW, Bloch RJ. Differential distribution of dystrophin and beta-spectrin at the sarcolemma of fast twitch skeletal muscle fibers. J Muscle Res Cell Motil. 1999b; 20:383–393. [PubMed: 10531619]

Winder S. The membrane-cytoskeleton interface: the role of dystrophin and utrophin. J Muscle Res Cell Motil. 1997; 18:617–629. [PubMed: 9429156]

Wojcikiewicz E, Zhang X, Moy V. Force and compliance measurements on living cells using Atomic Force Microscopy (AFM). Biol Proced Online. 2004; 6:1–9. [PubMed: 14737221]

Wolff AV, Niday AK, Voelker KA, Call JA, Evans NP, Granata KP, Grange RW. Passive mechanical properties of maturing extensor digitorum longus are not affected by lack of dystrophin. Muscle Nerve. 2006; 34(3):304–312. [PubMed: 16770793]

Zhang Q, Wang X, Wei X, Chen W. Characterization of viscoelastic properties of normal and osteoarthritic chondrocytes in experimental rabbit model. Osteoarthr Cartil. 2007; 16(7):837–840. [PubMed: 18032072]

Zubrzycka-Gaarn E, Bulman D, Karpati G, et al. The Duchenne muscular dystrophy gene product is localized in sarcolemma of human skeletal muscle. Nature. 1988; 333(6172):466–469. [PubMed: 3287171]

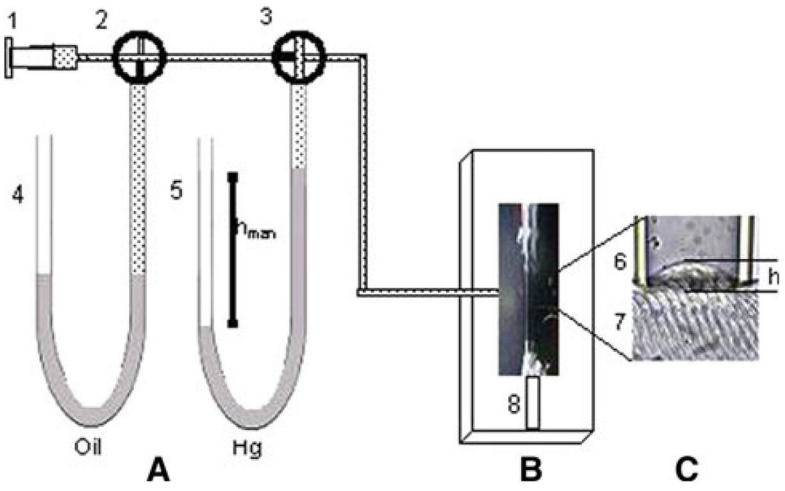

Fig. 1.

Experimental arrangement. The experimental system consisted of (*A*) a set of manometers, (*B*) the optical system (not shown) with a compound microscope to observe the isolated fiber, and (*C*) the bleb formed by the applied negative pressure P to the myofiber. The syringe (1) was connected to manometers filled with perfluorinated polyether manometer (4) or with mercury (5), which were used independently. We used 4 way key valves (2 and 3) to set P inside the syringe with either of the manometers. Also shown are the micropipette (6) and the surface of the isolated myofiber (7), attached to the bottom of the experimental chamber with a clip (8). We induced a bleb of variable height h in the surface of the fiber by applying suction pressure. When key valve 3 was open to the syringe through valve 2 (shown as closed to manometer 4 in the drawing) the syringe, manometer and micropipette had the same negative P. By closing the branch between key valve 3 and the syringe (as shown in the figure), P inside the manometer and the micropipette were the same and remained constant

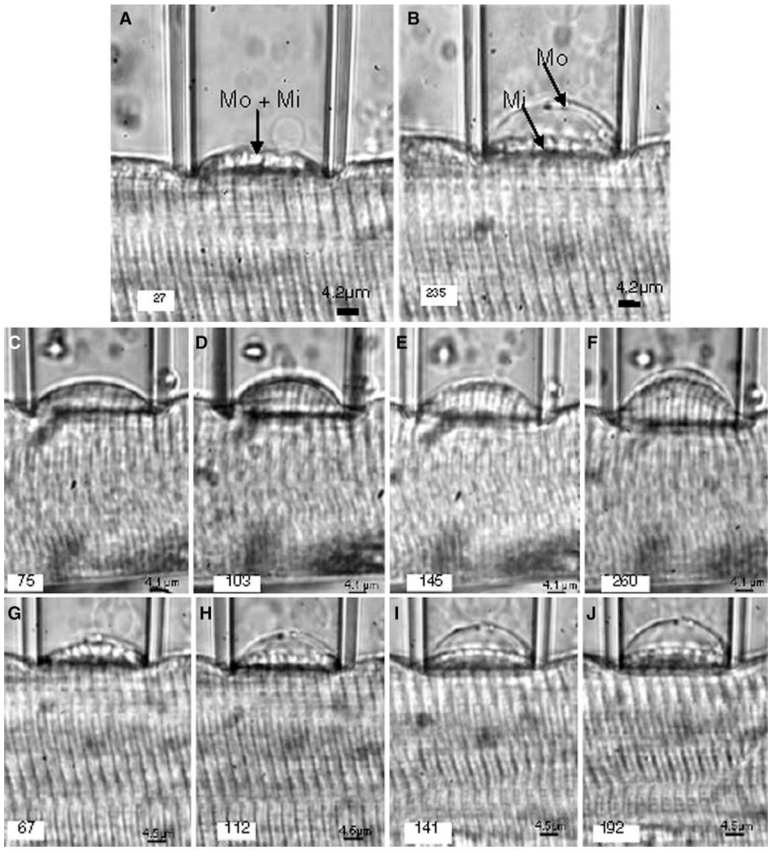

Fig. 2.

Induction of a sarcolemmal bleb by increasing suction pressure. **a**, **b** Two different suction pressures were applied sequentially to the sarcolemma of a *WT* myofiber isolated from the EDL muscle of a mouse. The pipette diameter was 26.6 µm and the fiber diameter was 55.1 µm. The fiber was stretched to an average SL of 3.2 µm. **a** The sarcolemma (M_o) and the contractile elements in the myoplasm (M_i) remained attached to each other as the bleb was sucked into the pipette at a pressure, $P = 27 \times 10^3$ dynes/cm^2. **b** At a higher suction pressure, $P = 235 \times 10^3$ dynes/cm^2, M_o was separated from M_i. As a result, the contractile apparatus lay well below the full height of the bleb within the pipette. The results show that the muscle cell surface developed tension due to the stretching and resistance to deformation by bending. **c**–**j** *Photomicrographs* of different blebs forming with progressively increasing pressures. Separation of M_o and M_i with increasing suction pressure, is shown in muscle fibers from *WT* with a SL = 3.3 µm (**c**–**f**) and *mdx* mice with SL = 3.4 µm (**g**–**j**). $P \times 10^3$ in dynes/cm^2 is indicated in the *left lower corner* of each photomicrograph. The results indicate that, at similar SLs and Ps, the distensibility of the *WT* muscle surface was considerably lower than that of *mdx* muscle. The *transparent lines* outside the surface of the bleb are due to *Becker lines* and therefore do not represent real structures

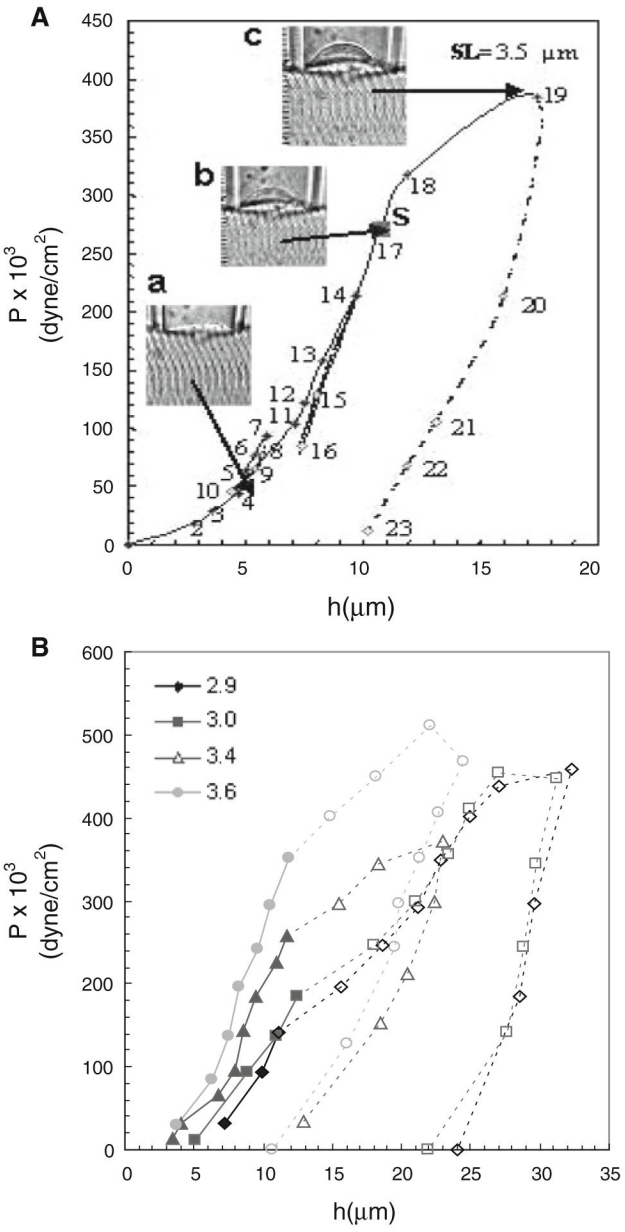

Fig. 3.

Pressure–displacement curve and effect of SL in a *WT* muscle fiber. **a** P was first increased in steps (*solid lines*) and then decreased (*dashed lines*). S denotes the pressure at which separation of the sarcolemma from the underlying contractile structures, P_{sep}, occurred (point 17). *Insets* Photomicrographs of the bleb: (*a*) point 4, without separation of the sarcolemma, M_o, from the contractile elements, M_i. (*b*) point 17, at which M_o separated from M_i. (*c*) point 19, at which pressure was further increased after separation occurred. The results show hysteresis after point 19. **b** Separation of the sarcolemma from the contractile elements depends on SL. Pressure–displacement curves were generated in different *WT* myofibers, each of which was stretched to the SL indicated in the *left upper corner* of the figure. *Filled symbols* joined with *solid lines* are the segments of the curves before

separation of the sarcolemma, M_o, from the contractile apparatus in the myoplasm, M_i. *Open symbols* joined with *dashed lines* are the remaining segments of the curves after separation of M_o from M_i. The results show that P_{sep} increases as SL increases

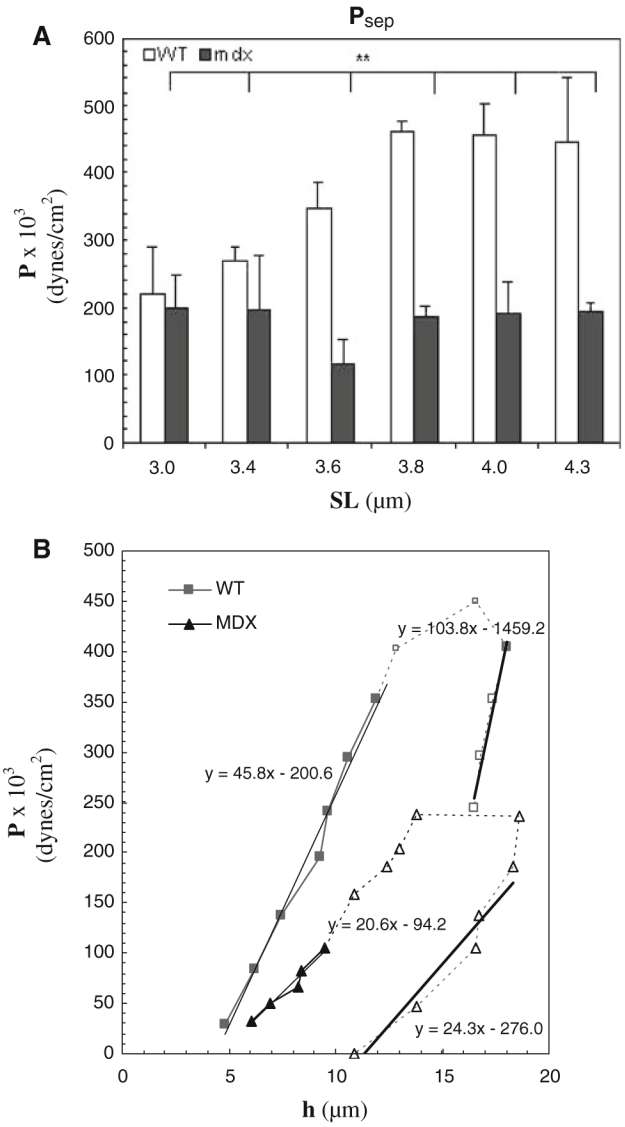

Fig. 4.

Effect of SL on separation pressure in *WT* and *mdx* myofibers. **a** P_{sep} was determined for *WT* and *mdx* myofibers. *Bars* indicate mean ± SD. ** indicates values significantly different from each other, $P < 0.01$. For all experiments ($n = 8$ for *WT; n* = 5 for *mdx*). In *WT* myofibers, the dependence of P_{sep} on SL was greater than in *mdx*. **b** Shift in the P–h curve in *WT* and *mdx* myofibers, stretched to an average SL of 3.5 μm. *Filled symbols* and *solid lines* represent data obtained before separation of the sarcolemma, M_o, from the contractile elements, M_i. *Open symbols* and *dashed lines* represent the data obtained after separation of M_o from M_i. S denotes the suction pressure at which separation occurred. The equations of the *regression lines* calculated from the equation, y = mx+b, are given next to each region of both curves. P_{sep} for *mdx* myofibers was smaller than for *WT,* indicating a weaker attachment of the sarcolemma to underlying contractile elements

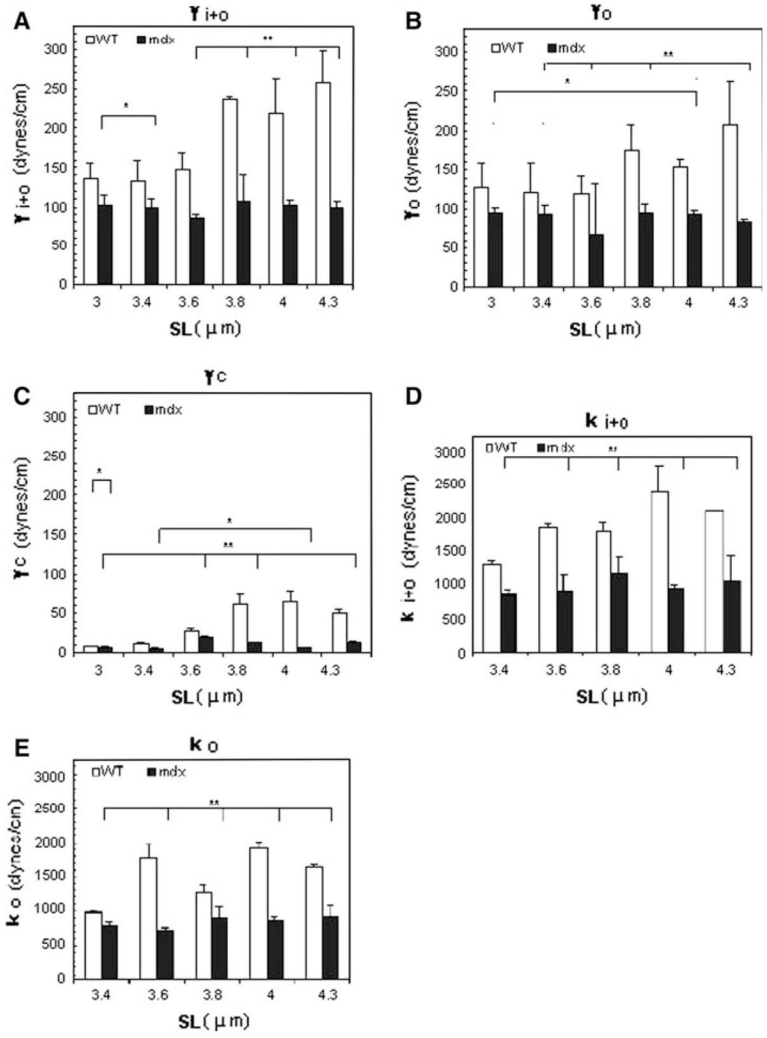

Fig. 5.

Surface tensions (γ) and stiffness (k) in *WT* and *mdx* myofibers as a function of SL. The figure shows *histograms* of tensions of the total system (γ_{i+o}, **a**), the sarcolemma (γ_o, **b**) and the maximal tension sustained by the costameres and associated structures (γ_c, **c**; see text) at different SLs in *WT* and *mdx* myofibers. The *mdx* fibers had consistently lower values for γ and showed no dependence of γ on SL. **d**, **e** Stiffness was computed from Hooke's Law. **d** k_{i+o}, stiffness sustained by the intact contractile apparatus–costameres–sarcolemma complex and **e** k_o, sarcolemmal stiffness, measured after separation of the sarcolemma. *Bars* indicate mean ± SD. Both values were lower in *mdx* than *WT* muscle fibers. ** indicates values significantly different from each other, $P < 0.01$ and * denotes values significantly different from each other, $P < 0.05$ ($n = 7$ for *WT* and $n = 5$ for *mdx*)

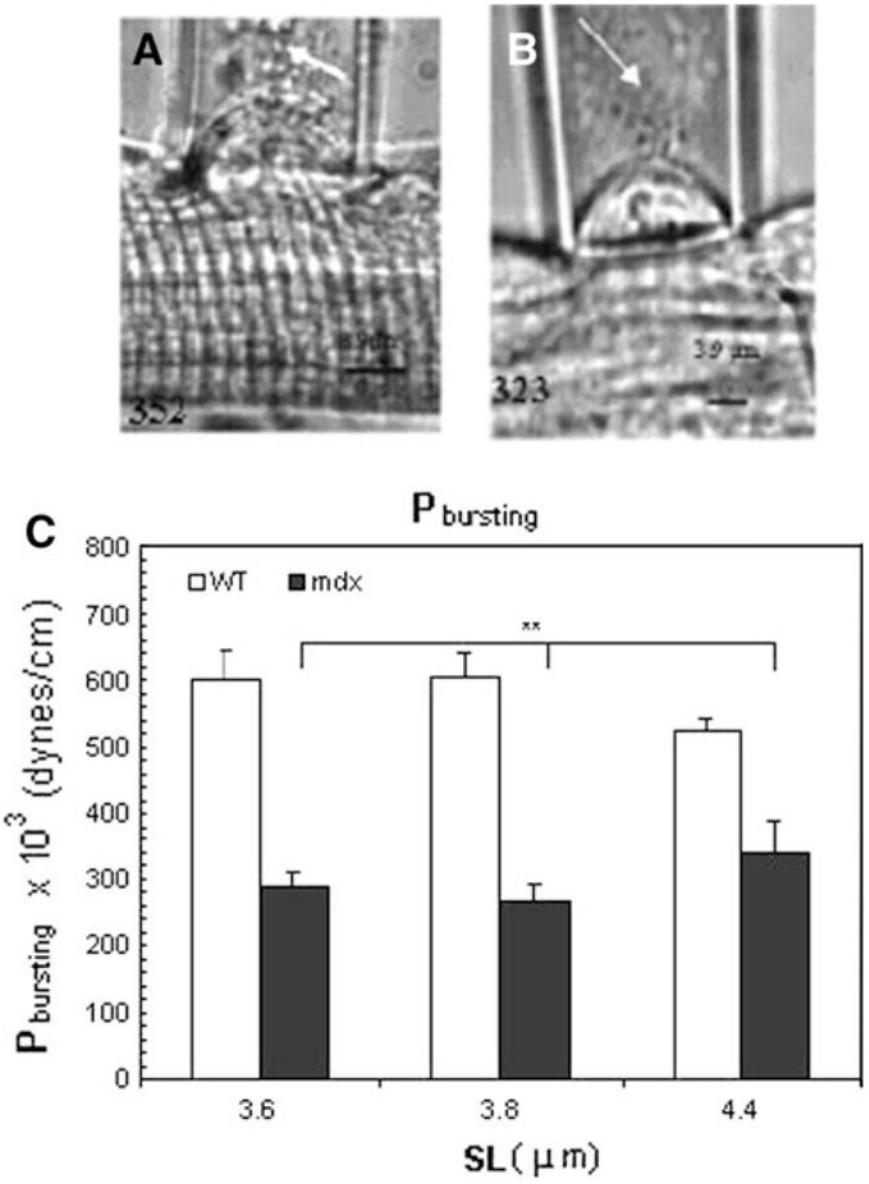

Fig. 6.

Bursting of the sarcolemmal bleb at large negative pressures. Increasing negative pressures were applied to the surface membrane of the myofibers after separation of the sarcolemma from the underlying contractile structures, until the surface membrane burst (*arrows*). **a**, **b** Myofibers from *WT* (**a**) were studied at SL = 3.2 μm and from *mdx* mice (**b**) at SL = 3.3 μm. Values for $P \times 10^3$, in dyne/ cm^2, at which each *photomicrograph* was taken, is given at the bottom of each image. **c** *Histograms* of bursting pressure $P_{bursting}$ as a function of SL. At all SLs studied, $P_{bursting}$ of myofibers from *WT* mice were approximately 2-fold higher than in *mdx* myofibers. *Bars* indicate mean ± SD; ** indicate values significantly different from each other, $P < 0.01$ ($n = 5$ for *WT* and $n = 3$ for *mdx*)

Table 1

P_{sep}, $P_{bursting}$, k, γ_{i+o}, γ_o and γ_c, and the population variances, $V_{\gamma i+o}$, V_o and $V_{\gamma c}$ expressed as mean ± SD, calculated from all SLs examined

	$P_{sep} \times 10^3$ (dynes/cm^2)	$P_{bursting}$ (dynes/cm^2)	k_{i+o} (dynes/cm^2)	k_o (dynes/cm^2)	γ_{i+o} (dynes/cm^2)	$V_{\gamma i+o}$	γ_o (dynes/cm^2)	V_o	γ_c (dynes/cm^2)	$V_{\gamma c}$
WT	367 ± 26	631 ± 47	1894 ± 142	1524 ± 96	188 ± 21	46 ± 5	151 ± 25	30 ± 4	37 ± 6	4 ± 1
mdx	171 ± 19*	321 ± 34*	989 ± 204*	846 ± 102*	99 ± 10*	2 ± 1	89 ± 14*	3 ± 1	11 ± 4*	1 ± 1

*Significant difference from control ($P < 0.05$ or lower)

J Muscle Res Cell Motil. Author manuscript; available in PMC 2015 February 12.